THE ASTROPHYSICAL JOURNAL, 296:90–105, 1985 September 1

A STATISTICAL STUDY OF THE RELATIONSHIP BETWEEN GALAXY INTERACTIONS AND NUCLEAR ACTIVITY[1]

ROC M. CUTRI AND CHRISTOPHER W. MCALARY
Steward Observatory, University of Arizona
Received 1984 December 19; accepted 1985 March 11

ABSTRACT

We have obtained small-aperture near- and mid-infrared photometry of a complete sample of interacting galaxies from the *Catalog of Isolated Pairs of Galaxies in the Northern Hemisphere* (Karachentsev 1972). Statistical comparison of the nuclear properties of these galaxies with samples of noninteracting galaxies shows that signs of abnormal nuclear activity are much more common in interacting systems. In particular, a population of nuclei with extremely luminous 10 μm emission is unique to the interacting sample. Roughly half of the interacting galaxies with nuclear 10 μm sources also exhibit evidence of extended 10 μm emission using measurements from *IRAS*. The far-infrared luminosities of the interacting sample are also greater than those of representative selections of normal galaxies. The identification of extraluminous infrared emission in a significant number of the surveyed galaxies suggests that interactions may in some way be associated with other high-luminosity phenomena such as Seyfert nuclei and QSOs.

Subject headings: galaxies: clustering — galaxies: nuclei — galaxies: photometry — infrared: sources

I. INTRODUCTION

It has become evident in recent years that there exists some relationship between galaxy interactions and the presence of abnormal activity. Larson and Tinsley (1978) were among the first to note this connection when they found that galaxies with optical colors consistent with recent bursts of star formation were nearly always part of interacting systems. Interacting galaxies tend to have enhanced radio emission (Sulentic 1976; Stocke, Tifft, and Kaftan-Kassim 1978; Condon and Dressel 1978; Hummel 1981; Condon *et al.* 1982), an abundance of optical emission lines (Heckman *et al.* 1983; Wasilewski 1983; Kennicutt and Keel 1984), infrared excesses (Rieke *et al.* 1980; Joseph *et al.* 1984; Lonsdale, Persson, and Matthews 1984), and strong far-infrared emission (Soifer *et al.* 1984*b*). Seyfert nuclei may occur more frequently in interacting and disturbed galaxies, or those in groups (Adams 1977; Davis 1981; Dahari 1984*a*). Even QSOs are now being found to have close and sometimes interacting companions (Bothun *et al.* 1982; Stockton and MacKenty 1983; Hutchings *et al.* 1984; Heckman *et al.* 1984).

We have undertaken a study of the infrared properties of a statistically complete sample of interacting galaxies chosen from the Karachentsev (1972) Catalog of Isolated Pairs of Galaxies in the Northern Hemisphere. The goal of this work is twofold. Larson and Tinsley (1978) noted the apparent connection between galaxy encounters and galaxy-wide star formation. Other observations, such as those of the *Infrared Astronomical Satellite* (*IRAS*), sample only the global star formation rate. This paper will address the question of the extent to which galaxy interactions influence *nuclear* activity. Such a study will allow us to probe how the origin, scale, and frequency of activity in galactic nuclei are related to interactions. This involves a statistical comparison of the observed incidence of activity in the interacting systems with those in a comparable selection of noninteracting ones.

The term "activity" is used in this work to describe the presence of an emission mechanism other than a normal galactic stellar population. In this context, active nuclei include those of Seyfert galaxies, low-ionization nuclear emission-line regions (Liners), and starburst galaxies, as well as nuclei with grossly abnormal stellar populations or large amounts of extinction. The specific nature of the active nuclei will be detailed in a later work.

The second goal of this work is to examine the mechanics of the interactions themselves. Using *n*-body simulations, Toomre and Toomre (1972), Miller and Smith (1980), and Negroponte and White (1983), along with a number of others, have explored the spectacular effects of gravitational encounters on the collective stellar geometries of galaxies. Unfortunately, little can be said of the dynamics of the nonstellar material in such encounters, which is the true tracer of nuclear activity. Consequently, we must rely on empirical techniques to probe the manner in which interactions manipulate gas and dust. In a following paper we will investigate which aspects of the interactions appear most to influence nuclear activity. This analysis will consider such properties as galaxy and interaction morphologies, separations, extent of the active regions, and the overall spectral energy distribution.

II. SAMPLE SELECTION

a) The Interacting Sample

Studies of interacting galaxies are often hampered by the lack of a statistically unbiased collection of sources. To a large extent, this problem stems from the uncertainty concerning just what an interacting galaxy is. It is attractive to examine only the more spectacular examples in the Atlas of Peculiar Galaxies (Arp 1966), for instance, but such subjective sampling techniques will bias any conclusions reached. In addition, observing only violent mergers provides no information on

[1] Some of the observations reported here used the Infrared Telescope Facility, which is operated by the University of Hawaii under contract from the National Aeronautics and Space Administration, and the Canada-France-Hawaii Telescope, operated by NRC Canada, CNRS, and the University of Hawaii.

how the degree of interaction affects the resulting continuum of activity. It is important to recognize that interacting systems occur with an incredibly diverse range of morphologies and number of participants, and the full range must be considered.

With the intent of minimizing the biases and simplifying the identification procedure, we have selected a sample of sources from the Catalog of Isolated Pairs of Galaxies in the Northern Hemisphere (Karachentsev 1972, hereafter CPG). The CPG contains 603 pairs of galaxies north of declination $-3°$, having photographic magnitudes brighter than $m_{pg} = 15.7$. The quality which makes the CPG an ideal source for our sample is that the pairs in the catalog were chosen to be physically associated on the basis of the galaxies' angular sizes and separations, not on a subjective assessment of their interaction. The CPG's selection criteria were devised to limit the number of optical pairs by selecting galaxies of comparable sizes. Each pair in the CPG has an assigned interaction morphology and subtype, denoted in the following way. LIN: those pairs which exhibit filamentary structure either in the form of connecting bridges (br) or tails (ta); ATM: pairs which are surrounded by a common atmosphere which is either symmetrical and amorphous (am) or asymmetrical and shredded (sh); DIS: pairs in which the spiral structure of one (1) or both (2) of the members is distorted; SEP: pairs that show no signs of interaction or distortion. These classifications offer a reasonably good guideline for recognizing interacting systems, and we have adopted them for that purpose, although they are clearly subjective (Stocke 1977).

Our sample consists of the subset of pairs in the CPG which lie in the declination range $0° \leq \delta \leq 37°$, in which each member of the pair has $m_{pg} \leq 14.5$ or the pair has a combined brightness of $m_{pg} \leq 13.8$, and which show clear signs of interaction. Initially, the CPG interaction morphology was used as a basic discriminator for this last requirement; we selected the LIN and DIS pairs because of their conspicuously disturbed morphologies. The only shortcoming of the CPG classifications is that they are based solely on the National Geographic Palomar Sky Survey prints. Therefore, all the pairs in the catalog, within the spatial and brightness limits, were reexamined either on the Sky Survey prints or, when available, on deeper or larger scale prints (Vorontsov-Velyaminov 1959, 1977; Arp 1966; Stocke 1977; Stocke, Tifft, and Kaftan-Kassim 1978). This visual assessment showed that the evidence for disruption in four DIS pairs, K186, K202, K333 and K356 was only marginal, and they were removed from our primary source list. Although the ATM pairs may share common structure, only the ATM(sh) subtypes were included in the sample because we felt that only these display true signs of tidal disruption. One ATM(am) pair, K46, was added because one of its components is actually a disturbed ring galaxy. Three SEP pairs were added because closer scrutiny showed that they were better described as DIS(1) or DIS(2); these were K125, K210, and K335. One pair within the sample limits, K343, was excluded because it is an optical pair (Tifft 1982). In Table 1A are listed the 39 pairs which comprise the final sample.

A number of other CPG pairs were observed in the course of this work, and they are listed in Table 1B. Most were of the LIN type, and will be used in further analysis on interaction types. This discussion will appear in a following work. These data are presented here separately, and are not used in the primary statistical arguments in this paper.

Using the CPG as a basis for a sample selection has many benefits. First, because the CPG deals with isolated pairs of galaxies, interactions can be investigated at their most fundamental level: the two-body interaction. Second, the catalog has been reviewed extensively for completeness and accuracy. Stocke (1977) examined the CPG, which claims to be complete to $m_{pg} = 15.7$, and found that within the definition of its selection criteria it is essentially complete to only $m_{pg} = 15.0$. Our subset is well within the domain of the complete sample. Individual galaxy and interaction classifications have also been screened by Stocke (1977), who obtained high-resolution images of many of the pairs. Tifft (1982) has obtained low-dispersion optical spectra of 370 of the closer pairs in the CPG, for the purpose of determining accurate relative redshifts. These velocity data have enabled the identification of optical pairs in the CPG.

Finally, a broad data base exists for many of the galaxies in the CPG. In addition to the optical spectroscopy of Tifft (1982) cited above, Stocke, Tifft, and Kaftan-Kassim (1978) have observed all 603 pairs at 11 cm to a detection limit of 40 mJy, and have made follow-up 6 cm and interferometric observations of the 11 cm detections. Neutral hydrogen data and radial velocities for 113 of the CPG pairs have been acquired by Davis and Seaquist (1983), who included them in their 21 cm line survey of interacting and isolated galaxies. The declination and magnitude limits we have set ensure that the galaxies in our sample were included in the Arecibo 2380 MHz continuum survey (Dressel and Condon 1978). Additional optical and infrared data are available for a number of the sources in our sample from the works of Keel *et al.* (1985), Dahari (1984*b*), Joseph *et al.* (1984), and Lonsdale, Persson, and Matthews (1984).

b) The Control Sample

To determine whether galaxy interactions are capable of inducing nuclear activity, we must compare the properties of interacting systems with those of noninteracting ones. We have drawn control groups for this comparison from the 10 μm surveys of bright spiral galaxies (Rieke and Lebofsky 1978) and Virgo spirals (Scoville *et al.* 1983), and the near-infrared studies of spirals and irregulars of Aaronson (1977) and of elliptical and S0 galaxies by Frogel *et al.* (1978). A small amount of overlap exists between these control surveys and our interacting lists. Any galaxies shared have been excluded from the comparison samples.

The surveys cited above also contain a number of other interacting systems not included in our sample. Such systems have been identified either as CPG pairs, or are listed as interacting in other catalogs such as the UGC or those of Arp (1966) and Vorontsov-Velyaminov (1959, 1977), or visually from the Palomar Sky Survey images. The data from these galaxies were not included in the comparison samples but were considered with the data of the additional interacting galaxies. Table 2 contains a list of the interacting systems found in the comparison samples, along with their source surveys and morphological properties.

A total of 93 galaxies make up the near-infrared control sample. This sample was constructed of a proportion of spiral and irregular galaxies to elliptical and S0 galaxies similar to that found in our interacting sample (S/I:E/S0 = 67:13). It is comprised of the 76 noninteracting S and I galaxies listed in Aaronson (1977) and 15 representative E and S0 galaxies from Frogel *et al.* (1978).

Both the *IRAS* survey of Shapley-Ames galaxies by de Jong

TABLE 1A

COMPLETE CPG SAMPLE OF INTERACTING GALAXIES

CPG	UGC	NGC/IC	Position	Interaction Type[a]	X_{12}[b]	A[c]	Type[d]	cz (km s^{-1})	Notes
13.....	365	169a	0034+43	DIS(1)	0.37	2.3	SAab	4938	Arp 282,
		169a				0.7	...	4795	b = Mrk 241
31.....	966	520a	0122+03	LIN(ta)	0.65	1.9	pec	2165	probable merger,
		520b				1.3	pec	2176	VV 231, Arp 157
46.....	1430	750	0155+33	ATM(am)	0.45	1.4	E pec	5325	VV 189, Arp 166
	1431	751				1.3	E pec	5337	
53.....	1555	I195	0201+14	LIN(br)	2.16	1.4	SAB0	3648	VV 309, Arp 209
	1556	I196				2.3	SB	3640	
83.....	2388	1143	0253−00	ATM(sh)	0.71	0.8	E	8514	VV 331, Arp 118,
	2389	1144				0.7	S ring	8714	should be DIS(1)
99.....	3063	1587	0428+01	DIS(1)	0.97	1.9	E1 pec	3522	Mrk 616, II Zw 12
	3064	1588				1.0	E1 pec	3452	
118.....	3541	2274	0644+34	LIN(ta)	1.93	2.3	E	5032	
	3542	2275				1.4	S	4888	
125.....	3708	2341	0706+20	SEP	2.57	1.1	pec	5148	should be DIS(1)
	3709	2342				1.3	S pec	5159	
140.....	3995	...	0741+29	LIN(br + ta)	0.54	0.8	S pec	4577	
						0.9	S pec?	4797	
175.....	4619	2672	0847+19	ATM(sh)	0.56	1.8	E1	4206	Arp 167
	4620	2673				0.9	E0 pec	3850	
181.....	4718	2719a	0857+36	DIS(1)	0.53	1.5	Im pec	3190	Arp 202
		2719b				0.5	Im pec	3104	
210.....	5183	2964	0940+32	SEP	6.15	2.9	SABbc	1213	Mrk 404, B2 0939+32B,
	5190	2968				2.3	I0	1414	should be DIS(1)
216.....	5265	3018	0947+01	DIS(2)	2.75	1.1	S	1869	
	5269	3023				2.3	SABcd pec	1872	
234.....	5617	3226	1021+20	LIN(br)	2.35	2.5	E2 pec	1275	VV 209, Arp 94,
	5620	3227				3.7	SABa pec	1200	b = Seyfert 1.2
236.....	5637	3239	1022+17	LIN(br + ta)	0.67	2.7	IBm pec	685	Arp 263, probably large,
						0.6	pec?	701	diffuse single galaxy
249.....	5931	3395	1047+33	ATM(sh)	1.40	1.8	SABcd pec	1626	VV 246, Arp 270,
	5935	3396				2.2	IBm pec	1630	possibly DIS(2)
257.....	6026	3454	1052+18	LIN(br)	1.12	1.4	SBc	1107	
	6028	3455				0.6	SABb ring	1105	
295.....	6621	3786	1137+32	DIS(2)	1.45	2.0	SABa pec	2712	Mrk 744, VV 228,
	6623	3788				1.7	SABab pec	2627	Arp 294
296.....	6630	3799	1138+16	DIS(2)	1.29	0.7	SBb pec	3206	VV 350, Arp 83
	6634	3800				1.7	SABb	3268	
311.....	6933	3991	1155+33	LIN(br)	0.40	0.6	Im pec	3290	Arp 313, in small group
						0.6	...	3102	
334.....	7508	4382	1223+18	DIS(1)	7.75	6.5	SA0 pec	758	Virgo Cluster
	7523	4394				3.3	SBb	914	
335.....	7535	4410a	1224+09	ATM	0.33	0.7	Sab pec	7392	
		4410b				0.6	E?	7570	
347.....	7777	4567	1234+12	ATM(sh)	1.3	2.6	SABbc	2208	VV 219, Virgo Cluster
	7776	4568				4.2	SABbc	2105	
348.....	7851	4614	1239+26	DIS(1)	2.30	1.0	SB0	4842	Arp 34, VI Zw 506
	7852	4615				1.5	Sc	4732	
350.....	7865	4631	1240+33	DIS(2)	32.05	14.3	SBd	609	Arp 281
	7907	4656				8.9	SBm pec	641	
353.....	7896	4647	1241+11	DIS(1)	2.57	2.8	SABc	1450	VV 206, Arp 116,
	7898	4649				6.7	E2	1095	Virgo Cluster
359.....	8037	4795	1253+08	LIN(br)	0.45	1.8	SBa pec	2642	
		4796				0.5	?	2545	
362.....	8098	4861	1257+35	DIS(1)	0.97	1.1	SBm	850	Mrk 59, Arp 266,
		I3961				2.8	I	902	I Zw 49
389.....	8641	5257	1337+01	LIN(br + ta)	1.4	1.5	SABb pec	6899	VV 55, Arp 240
	8645	5258				1.5	SAb pec	6686	

TABLE 1A—*Continued*

CPG	UGC	NGC/IC	Position	Interaction Type[a]	X_{12}[b]	A[c]	Type[d]	cz (km s^{-1})	Notes
404.....	8898	5394	1356+38	LIN(ta)	1.90	1.6	SBb pec	3515	VV 48, Arp 84,
	8900	5395				2.7	SAb pec	3516	I Zw 77
438.....	9560	...	1449+36	DIS(2)	4.05	1.0	pec	1206	VV 324
	9562					1.4	pec	1272	
468.....	9903	5953	1532+15	LIN(br)	0.77	1.7	SAa pec	1983	VV 244, Arp 91,
	9904	5954				1.5	SABcd pec	2012	a = Seyfert 2
472.....	10033	5994	1545+18	LIN(br + ta)	1.57	0.8	I?	3625	VV 16, Arp 72
		5996				1.7	SB	3364	
526.....	11048	6500	1745+18	DIS(1)	2.31	1.8	SAab	3216	
	11049	6501				1.4	SA0	3101	
590.....	12737	7731	2339+03	DIS(1)	1.39	1.3	SBa	2868	
	12738	7732				1.7	Sdm pec	2957	
591.....	12779	7752	2344+29	LIN(br)	2.00	2.8	I0	5049	VV 5, Arp 86,
	12780	7753				2.4	SABbc	5158	IV Zw 155
592.....	12808	7769	2349+20	DIS(1)	5.48	2.8	SAb	4199	
	12815	7771				2.4	SBa	4364	
602.....	12908	7805	2359+31	LIN(ta)	0.87	1.2	SAB0 pec	5101	VV 226, Arp 112,
	12911	7806				1.1	SAbc pec	5059	Mrk 333
603.....	12914	...	2359+23	DIS(2)	1.13	2.1	Scd pec	4654	VV 254, III Zw 125
	12915					1.5	Sb	4651	

[a] CPG interaction morphology (see text).
[b] Projected pair separation in arc minutes.
[c] Major axis diameter of galaxy in arc minutes.
[d] Morphological type of galaxy.
[e] Radial velocity of galaxy.

TABLE 1B

ADDITIONAL INTERACTING PAIRS OBSERVED

CPG	UGC	NGC/IC	Position	Interaction Type[a]	X_{12}[b]	A[c]	Type[d]	cz (km s^{-1})	Notes
23.....	688	382	0105+32	ATM(sh)	0.54	0.8	E0	5170	VV 193, Arp 331,
	689	383				1.9	SA0	5242	IV Zw 38, 3C 31
64.....	1810	...	0218+39	LIN(br + ta)	1.34	1.8	...	7598	VV 323, Arp 273
	1813	...				1.1	...	7469	
65.....	1814	...	0219+16	LIN(br + ta)	0.24	1.3	SABbc	4248	b = small knot at end
						1.3	...	...	of U1814 arm, M51 type
71.....	2057	978	0231+33	SEP	0.34	1.6	...	4896	
						0.7	...	4787	
97.....	2947	1507	0402−02	LIN(br)	0.92	2.5	SBm pec	770	b = small knot
						1.4	...	...	north of NGC 1507
119.....	3555	...	1647+26	LIN(br)	0.61	0.5	SABbc	5028	M51 type
						1.1	...	4566	
144.....	4030	...	0745+28	SEP	0.54	0.4	...	8387	
						0.4	...	8086	
156.....	4264	2535	0808+25	LIN(br + ta)	1.77	2.1	SAc pec	3979	VV 9, Arp 82
		2536				1.0	SBc pec	3938	
161.....	4383	I2338	0821+21	LIN(br)	0.72	0.7	SABcd pec	5300	Arp 247
		I2339				0.9	SBc pec	5248	
168.....	4541	2648	0840+14	LIN(br + ta)	2.40	3.8	Sa	1925	Arp 89
						1.4	...	...	
221.....	5339	...	0954+21	LIN(br + ta)	0.35	0.6	...	7222	
						0.5	...	7297	
254.....	5984	...	1050+30	LIN(br + ta)	1.18	1.0	...	10407	VV 233, Arp 107
						1.0	...	10316	
302.....	6778	3893	1146+49	LIN(br)	3.66	4.7	SABc	977	Ursa Major Cluster
	6781	3896				1.6	SB0 pec	980	

TABLE 1B—*Continued*

CPG	UGC	NGC/IC	Position	Interaction Type[a]	X_{12}[b]	A[c]	Type[d]	cz (km s^{-1})[e]	Notes
303.....	...	3894	1146+60	SEP	2.03	2.2	E4	3196	
		3895				1.4	SBa	3073	
310.....	6921	3985a	1154+49	LIN(br)	0.37	0.8	SBm	1068	Ursa Major Cluster
		3985b				0.9	...	...	b probably spot on arm
355.....	7938	4676a	1244+31	LIN(br + ta)	0.58	0.8	S0 pec	6825	VV 224, Arp 242
	7939	4676b				0.8	SB0 pec	6632	
369.....	8335	...	1314+62	LIN(br + ta)	0.57	0.5	Sc	9489	VV 250, Arp 506,
						0.5	Sc	9399	VII Zw 506
390.....	8677	5278	1340+56	LIN(br)	0.56	0.8	SAb pec	7603	VV 19, Arp 239,
	8678	5279				0.5	SBa pec	7739	Mrk 271, I Zw 69
406.....	8931	5410	1359+41	LIN(br)	1.12	1.5	SB	3836	VV 256
						0.8	I	3903	
418.....	9098	...	1411+46	LIN(br)	0.53	0.6	...	8175	
						0.7	...	8397	
466.....	9851	5929	1524+42	LIN(br)	0.49	1.6	Sab pec	2709	Arp 90, I Zw 112
	9852	5930				0.9	SABb pec	2839	
470.....	9913	I4553	1533+24	ATM(sh)	0.21	0.5	pec	5257	Arp 220,
		I4554				0.6	pec	5328	probable merger
504.....	10724	6306	1707+61	DIS(1)	1.40	1.1	SBab pec	3308	
	10727	6307				1.5	SB0 pec	3527	
508.....	...	...	1718+49	LIN(ta)	3.79	0.9	E0	7493	VV 10, Arp 102
						1.2	SABb pec	7425	
516.....	10855	6376	1725+59	LIN(br + ta)	0.59	0.6	...	8864	VII Zw 712
		6377				0.6	...	8872	
527.....	11055	...	1755+12	SEP	4.37	1.1	...	...	
	11057	...				2.0	....	...	
552.....	11680	...	2105+03	LIN(br + ta)	1.23	1.0	Sc	8110	II Zw 101
						0.6	...	8260	II Zw 102
557.....	11751	...	2127+11	LIN(br)	0.67	0.7	SB	8646	
						0.7	...	8665	
564.....	11958	7236	2212+14	ATM(am)	0.59	0.9	...	8212	Arp 169, II Zw 172,
		7237				0.9	...	7964	3C 442
575.....	12332	7469	2301+09	DIS(1)	1.32	1.6	S	5045	Arp 298, a = Seyfert
		I5283				0.7	E	4916	

[a] CPG interaction morphology (see text).
[b] Projected pair separation in arc minutes.
[c] Major axis diameter of galaxy in arc minutes.
[d] Morphological type of galaxy.
[e] Radial velocity of galaxy.

et al. (1984) and *IRAS* measurements of the bright spiral sample galaxies of Rieke and Lebofsky (1978) have been compared with the far-infrared properties of the CPG sample. Because the specific galaxies included in the Shapley-Ames survey are unknown, this survey can be used as a gauge only of the properties of galaxies in general, and not of those of noninteracting galaxies in particular.

c) *Selection Effects*

All of the control sample galaxies are taken from studies of bright, relatively nearby objects. They range in radial velocity between 0 and ~2000 km s^{-1}, with only a few objects at higher velocities. The interacting sample redshift distribution, shown in Figure 1, ranges uniformly from 0 to over 5000 km s^{-1}, with a few galaxies up to 8700 km s^{-1}. The different redshift ranges might introduce some bias as a result of different absolute magnitude distributions, but the control sample galaxies are all relatively bright, with m_{pg} generally ≤ 12.5 mag. The difference of a factor of roughly 2–3 in the mean distances of the control and interacting samples is more than compensated for by the fainter magnitude limit of our sample ($m_{pg} \leq 14.5$ mag). More important, however, because we are investi-

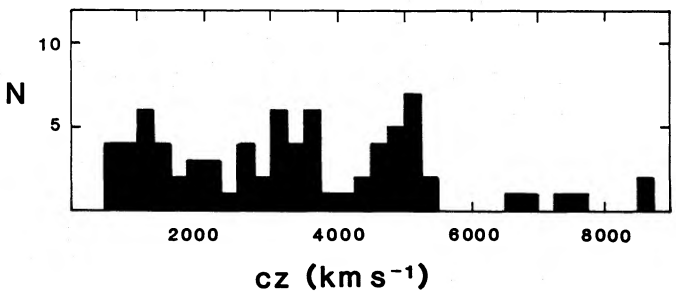

FIG. 1.—Radial velocity distribution of the primary CPG sample of interacting galaxies.

TABLE 2

INTERACTING GALAXIES FROM COMPARISON SAMPLES

Name (NGC)	CPG	Interaction Type	References	Notes
1097.....	...	...	1	not in CPG; interaction reference RCBG2
1232.....	...	...	1	not in CPG; interaction reference RCBG2
2146.....	110A	DIS(1)	2	
3031.....	218	DIS(1)	1, 2	CPG classified as SEP
3034.....				
3079.....	...	...	2	not in CPG; paired with NGC 3073
3607.....	278	SEP	3	
3608.....				
3627.....	...	...	2	not in CPG;
3628.....				interaction reference UGC
4298.....	332	...	4	
4302.....				
4490.....	341B	DIS(2)	1, 2	
5194.....	379	LIN(br)	1, 2	M51
5195.....				
5746.....	434B	SEP	2	
7332.....	570A	SEP	2	

REFERENCES.—(1) Rieke and Lebofsky 1978; (2) Aaronson 1977; (3) Frogel *et al.* 1978; (4) Scoville *et al.* 1983.

gating nuclear infrared properties, we are less susceptible to biases due to optical selection criteria. The 10 μm emission detected in nearly all galaxies except those few within or near the local Group is nonstellar in origin, and consequently is unrelated to the optical absolute magnitude of the galaxy.

The effects of the different redshift distributions will manifest themselves in two major ways: the dispersion of observed colors and the fraction of galaxies detected at 10 μm. In our analysis we have made use of near-infrared K-corrections for a standard elliptical galaxy's colors (Lebofsky and Eisenhardt 1985) and the observed 10 μm luminosity function of Virgo spiral galaxies (Scoville *et al.* 1983) to compensate for the different redshift ranges. In § IV, we will also discuss the possible effects of different projected aperture sizes on the observed flux levels and colors for galaxies at various distances.

The CPG, because it is comprised of pairs of galaxies, will be biased against certain types of interactions. Multiple systems, compact groups containing more than two galaxies, are generally excluded. Another class of object which may be undersampled in the CPG is the merger. If an interaction between galaxies has proceeded to the point where two distinct nuclei cannot be identified, then that system will probably not be included in the CPG. The catalog, however, does contain enough advanced mergers which are still distinguishable pairs that the class should be at least partially represented. One important colliding system with extraordinary infrared emission, IC 4553 (= Arp 220) is also the CPG pair K470. Other probable mergers in our sample include K31 (= NGC 520) and K236 (= NGC 3239).

III. OBSERVATIONS

Near-infrared photometry of the sample galaxies was obtained primarily at the University of Arizona Observatory (UAO) 1.55 m telescope on Mount Bigelow. The measurements were made through broad-band filters with effective wavelengths of 1.25 (J), 1.65 (H), and 2.2 (K) μm, using a liquid helium–cooled InSb photovoltaic detector system. Apertures with projected diameters of either 8".7 or 11".6 were used, and chopper throws ranging between 15" and 28" were used to reference areas of the sky north and south of the galactic nuclei. Additional J, H, K, and limited L (3.5 μm) photometry was obtained at the Canada-France-Hawaii Telescope (CFHT) through an 8" aperture, using the CFHT facility infrared photometer. Chopper throws of 15"–16" were used for these measurements.

Broad-band photometry at 10 μm was obtained at both the UAO 1.55 m telescope and the NASA Infrared Telescope Facility (IRTF) on Mauna Kea. The 1.55 m observations were made with the UAO liquid helium–cooled bolometer system, using 5".8, 8".7, or 11".6 apertures, and reference beams between 8" and 13" north and south of the nuclei. The IRTF observations were made with the facility bolometer. An aperture of 5".8 was used, along with a 10" north-south chopper throw. A complete log of all observations is given in Table 3.

The broad-band measurements were reduced against measurements of standard stars adopted from Elias *et al.* (1982), Campins, Rieke, and Lebofsky (1985), and Rieke, Lebofsky, and Low (1985). The absolute 10 μm flux calibration used was taken from Rieke, Lebofsky, and Low (1985). The standards were always observed through identical filters and apertures, and were chosen to be relatively close on the sky to the respective galaxies. The resulting observed magnitudes of the program galaxies are summarized in Table 4. Unless stated otherwise, the statistical errors in the measurements are ≤ 0.03 mag. No corrections for extinction in our Galaxy or redshift have been applied to the data in Table 4.

Mid- to far-infrared fluxes for the primary sample have been obtained from the *IRAS* Point Source Catalog. These in-band fluxes have been color-corrected as described in the *IRAS Explanatory Supplement* (Beichman *et al.* 1984), and have been listed in Table 5.

IV. DISCUSSION

a) 10 μm *Emission*

Because a normal galactic stellar spectrum declines steeply toward mid-infrared wavelengths, virtually any detection of 10 μm emission in all but the most nearby galaxies is indicative of

TABLE 3

LOG OF OBSERVATIONS

Number	Date (UT)	Telescope	Wavelength	Aperture (arcsec)	Throw (arcsec)	System[a]
1.....	1983 Mar 30–Apr 1	1.55 m	*JHK*	12	21–28	LHe InSb
2.....	1983 May 30–Jun 2	1.55 m	*JHK*	12	22–23	LHe Insb
3.....	1983 Nov15–18	1.55 m	*N*	8	8–10	UA bolometer
4.....	1984 Feb 24–28	1.55 m	*JHK*	12	15–24	LHe InSb
5.....	1984 Mar 16–20	IRTF	*N*	6	10	IRTF bolometer
6.....	1984 Apr 10	1.55 m	*N*	12	16	UA bolometer
7.....	1984 Apr 12–13	1.55 m	*JHK*	8	16–18	LHe InSb
8.....	1984 Apr 14	1.55 m	*N*	6	6–8	UA bolometer
9.....	1984 May 7–9	CFHT	*JHKL*	8	15–16	LN_2 InSb
10.....	1984 Jun 22	1.55 m	*N*	8	10–11	UA bolometer
11.....	1984 Aug 29–30	1.55 m	*JHKL*	12	22–33	LHe InSb
12.....	1984 Oct 14	1.55 m	*N*	12	12–13	UA bolometer
13.....	1984 Oct 28–30	1.55 m	*JHK*	8	23–24	LHe InSb
14.....	1985 Jan 5	1.55 m	*N*	12	15	UA bolometer

[a] LHe InSb = liquid helium-cooled InSb photovoltaic detector system; LN_2 = liquid nitrogen–cooled InSb photovoltaic detection system.

nonstellar radiation. Excess 10 μm emission, therefore, is a trademark of active nucleus objects such as Seyfert and starburst galaxies. In our survey, we have detected 22 of the 59 galaxies observed at 10 μm above the 2 σ detection level. Of the 59 observed, however, 42 have been measured to better than a 1 σ level of <16 mJy, the detection limit of the Virgo survey (Scoville *et al.* 1983). Nineteen of these have >2 σ detections. All of the galaxies which were detected have flux densities ≥ 16 mJy.

In Table 6 we have summarized the 10 μm detection rates of the primary sample CPG interacting galaxies, along with the additional observed sources. The rates are presented two ways: for the CPG sample as a whole, and as the fraction of galaxies observed to a 1 σ limit of 16 mJy. Also included is a breakdown of the interacting galaxies by broad morphological type. As expected, most of the detections of the CPG galaxies occur in spirals and irregulars. Only two elliptical galaxies were detected, K234a (= NGC 3226), the companion to the Seyfert 1.2 galaxy, NGC 3227, and K335b (= NGC 4410b).

Rieke and Lebofsky (1978) detected 44% of the 39 noninteracting bright galaxies they observed, and 38% of the 53 noninteracting Virgo spirals observed by Scoville *et al.* (1983) were detected at better than twice their 1 σ level of 16 mJy. At face value, the detection rates of the interacting and control samples are quite similar. However, as discussed earlier, the redshift distribution of the CPG sample is more heavily weighted toward higher redshift sources than the other samples. If the interacting galaxies follow the same 10 μm luminosity function as the Virgo spiral galaxies [$N(>S) \propto S^{-1}$; Scoville *et al.* 1983], then the fraction of detectable sources above the 16 mJy level should decrease as $N(S > 16 \text{ mJy}) \propto (cz)^2$. Figure 2 (*upper panel*) shows the fraction of CPG interacting galaxies detected as a function of radial velocity, along with the fraction expected on the basis of the Virgo 10 μm luminosity function. There is apparently an excess of sources detected over the predicted fraction at the higher redshifts. The number of observed sources in each velocity bin is small, however, resulting in correspondingly large uncertainties. Examining the detected fraction of all of the observed interacting galaxies with 1 σ levels of ≤ 16 mJy, as is done in Figure 2 (*lower panel*) improves the statistics, although the benefit of the complete sample is lost. Using the bin size we have chosen, the detection rates in both cases run only slightly greater than 1 σ above the corrected Virgo numbers. The excesses above the predicted Virgo numbers are consistent, however, and using a larger bin size increases their significance. This suggests that there is a real excess of galaxies in interacting pairs with bright nuclear 10 μm sources.

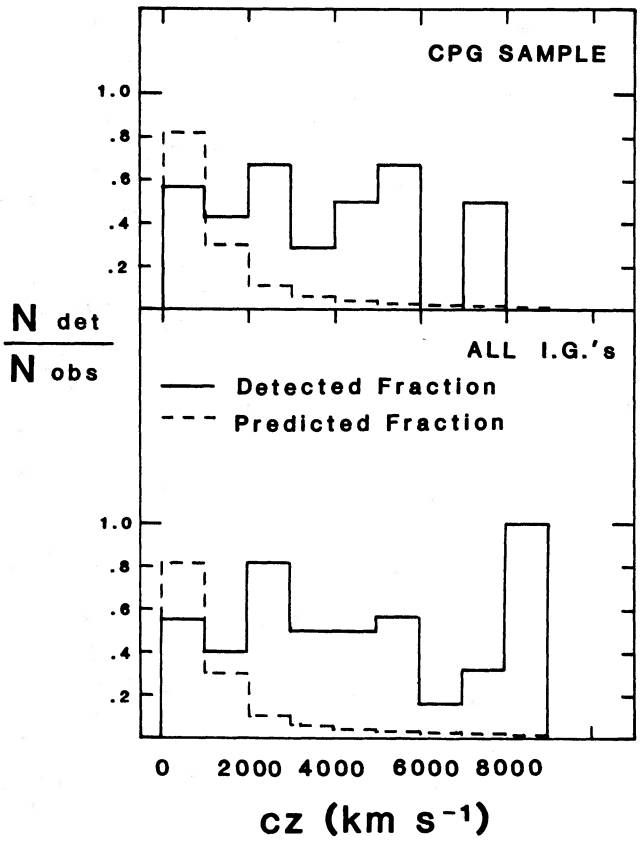

FIG. 2.—Fraction of galaxies detected at 10 μm as a function of radial velocity. Solid lines denote the fraction actually detected; dashed lines represent the predicted detection rate if the interacting galaxies follow the same 10 μm luminosity function as Virgo spiral galaxies. *Top:* results for the complete CPG sample; *bottom:* results for all of the interacting galaxies observed in this work.

TABLE 4A

OBSERVED MAGNITUDES OF THE CPG INTERACTING GALAXY SAMPLE

CPG	Observation Number	J	H	K	L	N	Notes[a]
13a.....	...	...	...	...	...	...	
b.....	...	...	...	...	...	...	
31a.....	...	9.39	8.48	8.58	...	4.73	*JHK* (1); *N* (2)
b.....	...	...	...	...	...	...	
46a.....	...	...	...	...	...	...	
b.....	...	...	...	...	...	...	
53a.....	3, 11	11.99	11.35	11.09	...	>5.78	
b.....	3, 11	11.87	11.20	10.93	...	>7.59	*N* (3)
83a.....	3, 11, 12	12.74	11.99	11.65	...	>6.13	
b.....	3, 11	12.23	11.48	11.07	...	>6.13	
99a.....	3, 12, 13	11.00	10.35	10.10	...	>9.00	
b.....	3, 12, 13	11.62	10.97	10.75	...	>7.91	
118a.....	4, 5	11.48	10.75	10.54	...	>8.65	
b.....	4, 5	12.48	11.75	11.55	...	>8.30	
125a.....	5, 13	11.76	11.15	10.89	...	6.83 ± 0.12	extended IR emission
b.....	5, 13	12.64	11.87	11.46	...	6.82 ± 0.10	
140a.....	4, 5	14.52:	14.26:	13.17:	...	>8.37	
b.....	4, 5	12.25	11.47	10.95	...	6.39 ± 0.10	
175a.....	4, 5	11.53	10.77	10.50	...	>8.90	*JHK* also (4)
b.....	4, 5	12.51	11.88	11.62	...	>8.40	
181a.....	5, 7	14.72::	14.15::	14.30::	...	>8.09	
b.....	5	...	...	...	...	>7.61	
210a.....	5, 9	12.29	11.40	11.08	10.47 ± 0.12	6.25 ± 0.10	
b.....	5, 9	11.40	10.64	10.40	10.23 ± 0.09	>8.41	
216a.....	5, 7	14.14:	13.46	13.23	...	>8.41	
b.....	5, 7	14.31::	14.06:	13.37::	...	>8.33	
234a.....	9	11.60	10.86	10.62	10.30±0.11	7.77 ± 0.42	*JHK* also (4)
b.....	9	10.99	10.20	9.68	8.79±0.05	5.27 ± 0.15	*N* (5), Seyfert 1.2
236a.....	5	...	...	...	...	>7.96	
b.....	...	...	...	...	...	...	
249a.....	4, 5	13.41:	12.70	12.51	...	7.83 ± 0.34	*N* peak 3″ NW optical nucleus
b.....	4, 5	12.96	12.25	12.11	...	7.00 ± 0.13	a, b: *JHK* also (6)
295a.....	5, 7, 9	12.09	11.33	10.81	9.70 + 0.14	7.06 ± 0.11	Seyfert 1; *JHKL* also (6)
b.....	5, 7	12.73	11.91	11.63	...	>8.24	*JHKL* also (6)
296a.....	5, 9	13.51	12.81	12.60	...	>8.82	a, b: *JHKL* also (6)
b.....	5, 9	12.61	11.84	11.50	...	7.73 ± 0.23	8″.3 NE: $N = 7.71 + 0.32$
311a.....	1	13.90:	13.40:	13.17:	...		
b.....							
334a.....	4, 5	10.31	9.64	9.54	...	>8.77	Virgo; *JHK* also (4)
b.....	5, 9	11.44	10.75	10.55	10.40 + 0.11	8.31 ± 0.55	*N* also (7)
335a.....	5, 9	12.98	12.25	11.97	...	>7.90	
b.....	5, 9	12.69	11.84	11.58	...	8.31 ± 0.55	
347a.....	4	12.79	12.07	11.90	...	>7.08	Virgo; *N* (7)
b.....	4	11.79	11.58	11.22	...	6.89 ± 0.32	*N* (7)
348a.....	7	12.46	11.82	11.43	...	...	
b.....	7	14.48:::	14.01::	13.23::	...	...	
350a.....	4, 5	13.11	11.61	11.91	...	<6.16	*JHK* also (1); *N* extended
b.....	5	...	...	...	...	>7.58	
353a.....	4	12.90:	12.16	11.97	...	>7.59	Virgo; *N* (7)
b.....	4, 8	10.23	9.38	9.27	...	>7.15	*JHK* also (4)
359a.....	7	11.87	11.28	10.96	...	...	
b.....	7	13.09::	12.37	12.10	...	...	
362a.....	7	14.23:::	13.69:	13.34::	...	...	
b.....	...	...	...	...	...	...	
389a.....	1, 5	13.19	12.59	12.29	...	>8.19	*JHKL* also (6)
b.....	5, 9	12.89	12.11	11.81	...	>7.99	*JHKL* also (6)
404a.....	4, 5, 9	12.13	11.28	10.89	10.18±0.14	5.68 ± 0.33	*JHKL* also (6)
b.....	4, 5	12.52	11.74	11.52	...	>9.40	*JHKL* also (6)

TABLE 4A—*Continued*

CPG	Observation Number	*J*	*H*	*K*	*L*	*N*	Notes[a]
438a.....	5, 7	14.20::	13.68:	13.51	...	>8.28	
b.....	5, 7	...	14.03:::	13.46::	...	>8.57	
468a.....	1, 5, 9	11.33	10.68	10.34	10.15 ± 0.13	6.84 ± 0.15	Seyfert 2
b.....	1, 5, 9	13.08	12.57	12.01	...	8.16 ± 0.51	*HKL* also (6)
472a.....	2	14.53:::	14.04:	13.79::	...	...	
b.....	2	13.00:	12.34	11.98:	...	...	
526a.....	11, 8	11.76	10.94	10.71	...	>6.78	
b.....	11, 8	12.09	11.27	11.03	...	>6.06	
590a.....	11	12.63	11.97	11.68	...	...	
b.....	11	14.78:	14.44:	14.08:	...	...	
591a.....	12	13.26	12.55	12.19	10.99 ± 0.40	6.20 ± 0.71	*JHKL* (6)
b.....	12	12.64	11.79	11.41	11.01 ± 0.20	>5.67	*JHKL* (6)
592a.....	3, 11	11.82	11.16	10.87	...	>5.90	
b.....	3, 11	11.61	10.79	10.28	9.15 ± 0.12	6.17 ± 0.17	IR peak 9″ W of optical nucleus
602a.....	12, 13	11.76	11.16	10.88	...	6.33 ± 0.69	*KL* also (6)
b.....	13	12.07	11.46	11.17	...	...	*HKL* also (6)
603a.....	3, 13	11.81	11.11	10.82	...	5.64 ± 0.48	
b.....	3, 13	12.61	11.98	11.25	...	>5.86	

[a] Numbers in parentheses refer to sources listed below.

REFERENCES.—(1) Aaronson 1977; (2) Condon *et al.* 1982; (3) Lonsdale, Persson, and Matthews 1984; (4) Frogel *et al.* 1978; (5) Rieke 1978; (6) Joseph *et al.* 1984; (7) Scoville *et al.* 1983.

TABLE 4B

OBSERVED MAGNITUDES OF ADDITIONAL INTERACTING GALAXIES

CPG	Observation Number	*J*	*H*	*K*	*L*	*N*	Notes[a]
23a.....	3	...	...	...	...	>5.92	
b.....	3	...	...	...	...	>6.39	
64a.....	13	12.63	11.97	11.64	...	...	
b.....	13	13.33	12.59	12.24	...	...	
65a.....	3	...	...	...	...	>5.88	
b.....	3	...	...	...	...	>5.32	
71a.....	11	11.42	10.72	10.44	...	...	
b.....	11	13.26	12.55	12.27:	...	...	
97a.....	3	...	...	...	...	>4.96	
b.....	...	...	...	...	...	...	
119a.....	3, 13	14.12	13.53	13.24	...	>5.69	
b.....	3, 13	13.03	12.41	12.15	...	>6.60	
144a.....	...	...	...	...	...	>7.36	*N* (Rieke, unpublished data)
b.....	...	...	...	...	...	...	
156a.....	1	12.99	12.47	12.23	11.58 ± 0.20	...	*L* (1); *JHK* also (1)
b.....	1, 14	13.42	12.90:	12.57	11.53 ± 0.20	6.61 ± 0.69	*L* (1); *JHK* also (1)
161a.....	1	14.04:	13.29	12.87	...	>7.33	*N* (Rieke, unpublished data)
b.....	1	13.53:	12.87	12.63	...	7.41 ± 0.25	*N* (Rieke, unpublished data)
168a.....	1	11.22	10.51	10.22	...	...	
b.....	1	13.39:	12.76:	12.48::	...	...	extended at *K*
221a.....	1	13.06	12.39	12.04	...	...	
b.....	1	12.68	12.06	11.82	...	...	
254a.....	1	13.84:	13.18	12.98	...	...	
b.....	1	13.35:	12.71	12.23	...	...	
302a.....	1	12.05	11.35	11.08	...	...	Ursa Major
b.....	...	...	...	...	...	...	
303a.....	9	13.31	12.61	12.42	...	6.47 ± 0.41	*N* (2) b
b.....	...	...	...	...	...	...	
310a.....	2	12.85	12.33	12.15	...	...	Ursa Major
b.....	...	...	...	...	...	...	

TABLE 4B—*Continued*

CPG	Observation Number	*J*	*H*	*K*	*L*	*N*	Notes[a]
355a.....	2	12.82:	11.94	11.48	10.54 ± 0.10	...	*L* (1); *JHK* also (1)
b.....	2	12.73	11.97	11.70	11.31 ± 0.21	>7.94	*L* (1); *N* (3); *JHK* also (1)
369a.....	2	13.69:	12.95::	12.55:	...	...	
b.....	2	13.46::	12.48	11.87	...	...	strong far-IR source
390a.....	1, 8	13.12	12.36	11.95	11.64 ± 0.20	>7.51	*L* (1); *JHK* also (1)
b.....	1, 8	13.63:	12.97	12.62	12.00 ± 0.15	>6.75	*L* (1); *JHK* also (1)
406a.....	2	13.74::	13.18:	12.86:	...	...	
b.....	2	15.87:::	15.12::	14.49:::	...	...	
418a.....	1	13.87:	13.32	13.17	...	...	
b.....	1	14.03:	13.48	13.07:	...	...	
466a.....	1, 8, 9	12.19	11.50	11.25	11.50 ± 0.19	7.28 ± 0.31	*JHKL* also (1)
b.....	1, 8, 9	11.87	11.08	10.74	10.11 ± 0.09	5.88 ± 0.15	*JHKL* also (1)
470a.....	5	12.64	11.55	10.86	...	5.58 ± 0.05	*JHKLNQ* (4)
b.....	...	...	...	...	...	...	
504a.....	7, 10	13.84:::	12.82	12.23:	...	>5.56	
b.....	10	...	...	...	...	>6.20	
508a.....	2	12.74:	12.12	11.64	...	...	
b.....	2	12.57	11.87	11.49	10.70 ± 0.20	...	*L* (1); *JHK* also (1)
516a.....	2	14.07::	13.66:	13.31::	...	...	
b.....	2	12.40	11.71	11.44	...	...	
527a.....	11	13.32	12.66	12.34	...	...	
b.....	11	13.18	12.53	12.19	...	...	
552a.....	2, 10	12.84	12.14	11.61	...	5.72 ± 0.68	
b.....	2, 10	13.09	12.37	11.91	...	4.76 ± 0.37	
557a.....	2	13.36	12.82	12.51	...	...	
b.....	...	...	...	...	...	...	
564a.....	11	12.25	11.67	11.28	...	...	
b.....	11	12.80	12.35	11.79	...	...	
575a.....	...	11.19	10.20	9.57	8.47	...	*JHKL*, (5)
b.....	13	12.99	12.12	11.74	...	...	

NOTE.—All errors reflect the statistical uncertainties in the measurements. Unless otherwise stated, the errors in the *JHK* magnitudes are ≤0.03 mag; : = 0.03–0.05 mag, :: = 0.05–0.07 mag, ::: = >0.07 mag. The uncertainties in the *L* and *N* measurements are stated explicitly.

[a] Numbers in parentheses refer to sources listed below.

REFERENCES.—(1) Joseph *et al.* 1984; (2) Condon *et al.* 1982; (3) Lonsdale, Persson, and Matthews 1984; (4) Rieke *et al.* 1985; (5) Cutri *et al.* 1984.

TABLE 5

COLOR-CORRECTED *IRAS* FLUX DENSITIES OF THE CPG SAMPLE

CPG	12 μm	Uncertainty	25 μm	Uncertainty	60 μm	Uncertainty	100 μm	Uncertainty	Notes
13a.....	<0.46	...	<0.42	...	0.91	F	3.51	D	May be both galaxies
b.....	...	...	...	...	...	...	...	...	
31a.....	0.94	D	3.20	C	33.56	D	47.89	D	merger—both galaxies
b.....	...	...	...	...	...	...	...	...	
83a.....	...	...	...	...	...	...	...	...	no detections
b.....	0.33	C	0.75	C	5.62	C	12.05	C	
125a.....	0.57	E	0.76	C	5.48	D	14.77	F	
b.....	0.55	C	1.02	C	5.87	D	12.71	E	
140a.....	<0.26	...	0.44	E	0.68	C	2.00	C	may be both galaxies
b.....	...	...	...	...	...	...	...	...	
181a.....	<0.25	...	<0.25	...	1.99	C	2.52	C	may be both galaxies
b.....	...	...	...	...	...	...	...	...	
210a.....	0.78	B	1.45	C	12.54	C	23.59	C	
b.....	...	...	...	...	...	...	...	...	no detections
216a.....	...	...	...	...	...	...	...	...	no detections
b.....	<0.25	...	<0.32	...	2.33	C	4.95	C	
234a.....	...	...	...	...	...	...	...	...	no detections
b.....	0.81	B	1.88	C	8.34	C	17.19	D	

TABLE 5—*Continued*

CPG	12 μm	Uncertainty	25 μm	Uncertainty	60 μm	Uncertainty	100 μm	Uncertainty	Notes
236a.....	<0.25	...	<0.32	...	3.69	C	6.15	C	may be both galaxies
b.....	...	...	...	...	...	...	...	...	
249a.....	...	...	...	...	...	...	...	...	may be both galaxies,
b.....	<0.25	...	0.77	D	8.61	C	16.50	C	or between
257a.....	...	...	...	...	...	...	...	...	no detections
b.....	<0.30	...	<0.40	...	1.05	C	<2.22	...	
295a.....	...	...	...	...	...	...	...	...	not observed
b.....	...	...	...	...	...	...	...	...	not observed
296a.....	...	...	...	...	...	...	...	...	no detections
b.....	<0.34	...	0.57	D	5.13	D	11.69	D	
311a.....	<0.25	...	<0.29	...	2.78	D	4.69	D	may be both galaxies
b.....	...	...	...	...	...	...	...	...	
334a.....	...	...	...	...	...	...	...	...	no detections
b.....	<0.30	...	<0.25	...	1.06	C	4.24	D	
347a.....	...	...	...	...	...	...	...	...	no detections
b.....	0.67	C	1.01	D	16.82	D	47.08	...	
348a.....	...	...	...	...	...	...	...	...	no detections
b.....	<0.25	...	<0.27	...	1.23	C	3.24	D	
350a.....	2.12	C	3.10	D	55.60	D	119.80	C	
b.....	<0.69	...	<0.34	...	2.33	E	6.20	D	
353a.....	0.47	C	0.58	D	5.30	D	15.59	D	
b.....	...	...	...	...	...	...	...	...	no detections
362a.....	<0.25	...	0.51	D	1.92	D	2.31	C	may be both galaxies
b.....	...	...	...	...	...	...	...	...	
389a.....	0.68	C	1.42	C	10.91	D	18.32	D	
b.....	...	...	...	...	...	...	...	...	no detections
404a.....	<0.33	...	1.11	C	7.62	C	11.91	D	
b.....	...	...	...	...	...	...	...	...	no detections
438a.....	<0.25	...	<0.25	...	0.77	C	1.42	C	
b.....	...	...	...	...	...	...	...	...	no detections
468a.....	0.67	B	1.16	B	11.25	C	20.11	C	
b.....	...	...	...	...	...	...	...	...	no detections
472a.....	...	...	...	...	...	...	...	...	no detections
b.....	<0.25	...	0.67	C	4.41	C	7.42	C	
526a.....	<0.25	...	<0.25	...	0.78	C	2.60	C	
b.....	...	...	...	...	...	...	...	...	no detection
590a.....	...	...	...	...	...	...	...	...	no detection
b.....	<0.25	...	<0.29	...	0.78	D	2.61	D	
591a.....	...	...	...	...	...	...	...	...	may be both galaxies
b.....	<0.29	...	5.88	F	5.17	D	9.58	D	
592a.....	<0.41	...	0.73	D	5.11	C	11.41	D	
b.....	0.82	C	1.86	C	19.26	C	38.46	D	
603a.....	<0.38	...	<0.67	...	5.78	D	14.11	D	may be both galaxies
b.....	...	...	...	...	...	...	...	...	

NOTE.—All fluxes in janskys (10^{-26} W m^{-2} Hz^{-1}). The uncertainties are as given in the *IRAS* point-source catalog: A: uncertainty = 0%–4%, B: uncertainty = 4%–8%, C: uncertainty = 8%–12%, D: uncertainty = 12%–16%, E: uncertainty = 16%–20%, F: uncertainty > 20%.

At redshifts greater than 2000–3000 km s^{-1}, the excess of 10 μm bright nuclei implies that interacting galaxies will be detected exclusively. This effect may explain why interacting galaxies seem to be "overrepresented" in infrared selected samples of galaxies from *IRAS* data (Soifer *et al.* 1984*a*; Aaronson and Olszchewski 1984; Lonsdale, Neugebauer, and Soifer 1984). At some level, noninteracting Seyfert galaxies will also contribute to the number of higher redshift detections.

The abundance of extraluminous nuclei is quantitatively illustrated by the 10 μm luminosity functions of the interacting and control samples. The observed *N*-magnitudes listed in Table 4 have been converted to 10 μm luminosities using the bandpass of the *N* filter ($\Delta\lambda = 5$ μm), and a distance either from a published value (Aaronson *et al.* 1982; Aaronson and Mould 1983), from cluster membership, or from the use of an adopted Hubble constant of 82 km s^{-1} Mpc^{-1} (Aaronson and Mould 1983). The 10 μm luminosities of the bright spirals and Virgo spirals were derived in a similar fashion, using the fluxes of Rieke and Lebofsky (1978) and Scoville *et al.* (1983). Mean distances of 16.4 and 17.0 Mpc were assumed for the Virgo and Ursa Major Clusters respectively. Figure 3 displays the luminosity distributions of the interacting and bright galaxy

TABLE 6

TEN MICRON DETECTION RATES

Sample	Number Observed	Number Detected ($>2\ \sigma$)	Percent Detections
CPG Interacting Galaxies			
E/S0	10	2	20.0
Spirals	36	15	42.0
Irregulars	9	3	33.3
Total	55	20	36.4
CPG Interacting Galaxies ($1\ \sigma < 16$ mJy)			
E/S0	6	2	33.3
Spirals	30	15	50.0
Irregulars	8	3	37.5
Total	44	20	45.5

samples. Upper limits were included for the interacting sources which had 1 σ levels of ≤ 16 mJy. All upper limits are denoted by open squares.

The luminosity distribution of the interacting galaxy sample appears bimodal. Among the galaxies with detected 10 μm emission, there is an underlying population which is quite similar to the bright spiral sample. This base population ranges in luminosity up to perhaps $7 \times 10^8\ L_\odot$. The bright spiral distribution spans a similar range up to $\sim 4 \times 10^8\ L_\odot$. There are more low-luminosity detections among the bright spirals simply because of the larger number of low-redshift galaxies in the sample. These nearby low-luminosity sources will be more likely to be detected given a finite detection flux level. Virgo spirals, as discussed by Scoville *et al.* (1983), also occupy this same luminosity range. Their brightest 10 μm source, the Seyfert 2 galaxy, NGC 4388, has a luminosity of $4.8 \times 10^8\ L_\odot$. The large number of upper limits suggests that none of the distributions have sharp lower limits. It is likely that they extend smoothly to lower luminosities, where they merge with a third population: those galaxies whose 10 μm emission is purely stellar.

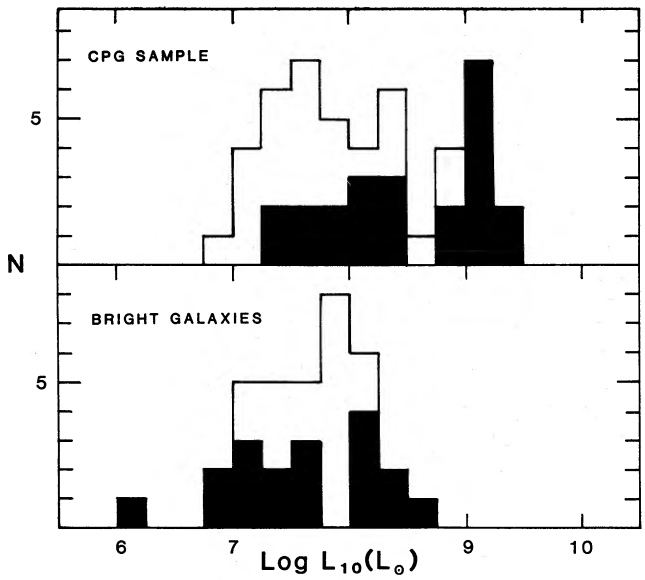

FIG. 3.—Ten micron luminosity distributions of the complete CPG sample of interacting galaxies (*top*) and the bright spiral galaxy sample of Rieke and Lebofsky (1978) (*bottom*). Open boxes represent 2 σ upper limits. Upper limits for the CPG sample have been included only when the 1 σ level is ≤ 16 mJy.

The feature which distinguishes the 10 μm luminosity function of the interacting galaxies from both bright spiral and Virgo samples is the luminous secondary poulation at $\sim 10^9\ L_\odot$. Approximately one-fourth of all the observed interacting systems occupy the luminous peak. Its mean luminosity exceeds that of the base distribution by a factor of ~ 20. The individual galaxies that make up the luminous population will be discussed in detail in another paper, but as a whole they are not distinct from others in the sample in terms of interaction morphologies.

It is unlikely that the detection of the extraluminous sources in the interacting sample is the result of some selection or observational bias. Any distance-related selection effect will tend to influence the lower end of the luminosity functions. High-luminosity sources will be equally detectable in both samples, if they exist. One of the more luminous nuclei at 10 μm, M82, is quite nearby, but it is part of the interacting pair K218. The luminous CPG galaxies are not preferentially the most distant sources in the sample. Rather, they span the same radial velocity range as the sample as a whole.

Another factor which may influence the relative observed 10 μm flux levels is the distance dependence of projected aperture diameters. Because the interacting sample is, on average, 2–3 times more distant than the control samples, we sample 4–9 times the surface area. Galaxies do not have uniform surface brightnesses at 10 μm, however. The 10 μm flux levels of galactic nuclei are generally observed to increase linearly with the aperture diameter, rather than as the square of the diameter (Rieke 1976). This would introduce a factor of 3, at best, in the mean luminosity of the CPG sample, if it were not for the fact that the sizes of galactic nuclei at 10 μm generally range from 150 to 600 pc (Rieke 1976). For those galaxies more distant than ~ 20 Mpc ($cz > 1650$ km s^{-1}), the nuclei will fall completely within the observing beam, essentially negating any aperture effect. As we shall argue below, the mean 10 μm surface brightnesses of galactic disks are much lower than the nuclei, so little contribution from them will be added to our relatively small aperture measurements. We can conclude, therefore, that the population of high-luminosity nuclei observed among the interacting galaxies is not an artifact of selection or observational biases.

To test the significance of the difference between the CPG and bright spiral 10 μm luminosity distributions, we have made use of the Gehan two-sample test, as described by Feigelson and Nelson (1985). This statistical experiment is designed to test the hypothesis that two distributions are the same, even when those distributions contain a significant amount of censored data (upper limits in this case). Applied to the two-luminosity distributions, the Gehan statistics confirm that they are different at the $\sim 98\%$ confidence level. If the data for all of the interacting galaxies are considered, including those culled from the bright spiral and Virgo samples, then the confidence level distinguishing interacting and noninteracting distributions is $> 99.9\%$.

It is clear that the distinction between the samples lies at the high luminosities. The bright galaxy sample's luminosity distribution can be taken to give the *a priori* probability that a normal galaxy will have a 10 μm luminosity $\geq 10^9\ L_\odot$. Because upper limits in both samples imply luminosities significantly less than $10^9\ L_\odot$, they may simply be counted with the lower

luminosity detections. Given that only one of the 39 noninteracting bright spirals is so luminous, the probability of observing 10 out of 49 normal galaxies in that range is $\sim 6 \times 10^{-6}$. Because this bright peak is not observed in samples of noninteracting galaxies, we must conclude that interactions, at least in isolated pairs of galaxies, are somehow capable of inducing activity which results in extremely large nuclear 10 μm luminosities. It is not clear, however, whether the interactions actually trigger new activity, or amplify the existing low-level activity which is present in a large fraction of normal galaxies (Rieke and Lebofsky 1978; Scoville *et al.* 1983). Amplification might occur if the interactions were able to provide more efficient fueling of a central engine, whereas new activity might result through the tidal disruption of previously stable nuclei.

b) *IRAS Fluxes*

Although this work emphasizes the nuclear emission from interacting galaxies, there is evidence for considerable extended infrared emission from a number of sources. Global infrared emission is sampled by the large-aperture measurements of *IRAS*, and about half of the CPG sample has been detected at one or more wavelengths in the *IRAS* all-sky survey. A measure of the strength of the extended component of the 10 μm light relative to the nuclear component is given by the ratio of the *IRAS* flux density (F_G) and small-aperture ground-based flux density (F_N). This ratio (F_G/F_N) is listed in Table 7 for the CPG sample. The large-aperture 10.4 μm flux densities have been estimated by extrapolating the 12 and 25 μm *IRAS* flux density levels. Upper limits are given in Table 7 for those sources which were detected in our observations, but not by *IRAS* and lower limits are quoted when the opposite applied. No ratio is listed for the galaxies which were not detected by *IRAS* or by ground-based observations.

Little can be inferred from the large upper limits in Table 7. Of those sources for which there are firm ratios, lower limits, or small (<2–3) upper limits, however, roughly half have at least as much emission emanating from their extranuclear regions as from within the nuclei themselves. This same proportion holds for just those galaxies with extraluminous nuclear 10 μm emission. Galaxies in our sample with more moderate nuclear 10 μm sources tend to have larger values of F_G/F_N. This tendency is probably a selection bias, however, because *IRAS* is less likely to have detected galaxies with lower luminosity disk emission.

TABLE 7

EXTENDED 10 μm EMISSION STRENGTHS AND 80 μm LUMINOSITIES

CPG	F_G/F_N	log L_{80} ($L_\odot$)	CPG	F_G/F_N	log L_{80} ($L_\odot$)
13	...	9.95	347b	9.8	10.00
31	1.6	10.58	348b	...	9.94
83b	>2.7	11.05	350a	15.9	9.77
			b	...	8.46
125a	8.0	10.66	353a	>13.7	9.51
b	7.3	10.63			
140	<2.4	9.70	362	...	8.44
181	...	9.58	389a	>31.0	11.06
210a	6.1	9.73	404a	<2.2	10.32
216b	...	9.34	438a	...	8.46
234a	<8.9	...	468a	7.0	10.01
b	2.5	9.46			
236	...	8.61	472b	...	10.09
249b	<2.4	9.76	526a	...	9.46
257b	...	<8.53	590b	...	9.39
296b	<11.0	10.18	591a	<2.1	...
			b	<2.8	10.52
311	...	9.81	592a	...	10.41
			b	5.7	10.95
334b	<17.5	8.92	602a	<1.7	...
335	<19.4	...	603a	<1.9	10.57

It must be noted that the *IRAS* measurements sample nearly 100 times the area of ground-based measurements. Therefore, even though there may be considerable 10 μm emission emanating from the galactic disks, in those galaxies with detected nuclear emission the mean surface brightnesses of the extranuclear regions are significantly lower than in the nuclei.

The extended 12 μm emission detected by *IRAS* is perhaps the best evidence for large-scale star formation because a compact "central engine" cannot readily power mid-infrared emission arising at such great distances from it (see, e.g., Cutri *et al.* 1984). The connection between interactions and galaxy-wide star formation corroborates the conclusions of Larson and Tinsley (1978), and the far-infrared *IRAS* observations further substantiate the distinctions between interacting and noninteracting galaxies. The overall mean 80 μm luminosity of the Shapley-Ames galaxies surveyed by de Jong *et al.* (1984), corrected to a Hubble constant of $H_0 = 82$ km s^{-1}, is $\sim 5 \times 10^9\ L_\odot$. The 80 μm luminosities of the CPG sample have been evaluated in the same manner as those of the Shapley-Ames galaxies, and are also listed in Table 7. The mean luminosity of the CPG galaxies is $(2 \pm 0.5) \times 10^{10}\ L_\odot$, a factor of 4 larger than the Shapley-Ames mean. Similarly, the mean 80 μm luminosity of the bright spiral galaxy sample is $(3 \pm 0.8) \times 10^9\ L_\odot$, which is consistent with the Shapley-Ames galaxies, and which emphasizes the evidence for enhanced infrared emission from the CPG sample galaxies. The more intense far-infrared emission in many interacting galaxies is almost certainly due to enhanced star formation throughout the systems.

c) *The Near-Infrared Colors*

Galaxies whose near-infrared light is dominated by the emission of a normal galactic stellar population have a narrow, well-defined range of near-infrared colors. Elliptical and S0 galaxies best exemplify this. Virtually all those measured by Frogel *et al.* (1978) have colors within a range of $0.8 \leq J-K \leq 1.2$. Their color distribution is sharply peaked near $J-K = 0.90$–0.95 mag. Any galaxy whose color falls outside that range either suffers from considerable extinction or has emission arising from sources other than a normal stellar population. Such alternative sources include an abnormal population of stars such as might result after a recent burst of star formation, or nonstellar sources, such as hot dust grains, ionized gas producing free-free emission, or a nonthermal source.

In Figures 4 and 5 we have constructed the corrected $J-K$ and $H-K$ color distributions of the interacting and noninteracting (cf. § II*b*) samples. K-corrections, as derived for a standard elliptical galaxy spectrum by Lebofsky and Eisenhardt (1984), have been applied to the colors of the interacting galaxies to provide first-order compensation for the different redshift distributions of the samples. Reddening in our own Galaxy has been corrected for by adopting the visual extinction estimates of Burstein and Heiles (1984) and the interstellar reddening curve of Rieke and Lebofsky (1985).

The color distributions of the two samples are superficially very similar. They are both dominated by a maximum occurring between 0.9 and 1.0 mag in $J-K$ and 0.1 and 0.3

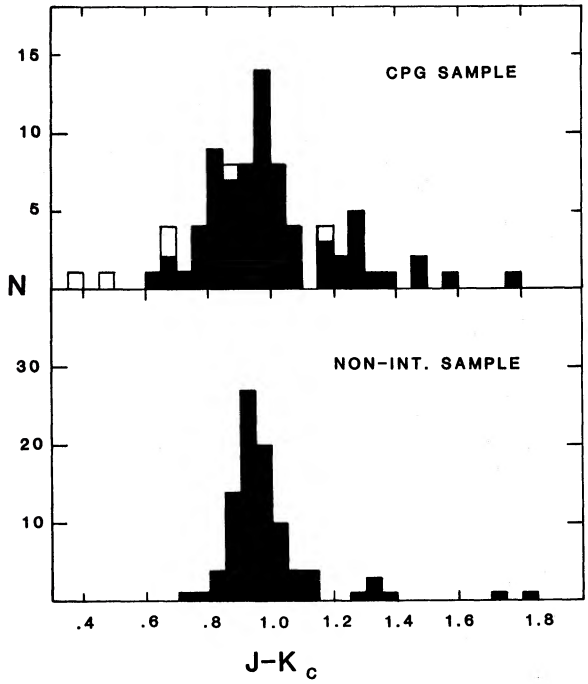

FIG. 4.—$J-K$ color distributions of the complete CPG sample of interacting galaxies (*top*) and noninteracting sample (*bottom*). Open boxes represent galaxy colors which have uncertainties of 0.07 mag or larger. All colors have been corrected for redshift, and for reddening in our Galaxy.

mag in $H-K$, and both possess definite tails to the red and to a lesser extent to the blue. The tails in the noninteracting distribution are nominally due to the contribution of spiral and irregular galaxies. As evidenced by the 10 μm luminosity function, some fraction of normal galaxies can be expected to exhibit signs of nuclear activity, in this case abnormal $J-K$ and $H-K$ colors. By far the largest fraction of galaxies in both distributions occupy the range expected for normal galaxies. However, the fraction of galaxies outside the "normal" range in the interacting sample is nearly a factor of 3 larger than in the noninteracting sample.

The higher dispersion in the colors of the interacting sample is not the result of large uncertainties in our measurements, or color-aperture effects arising from the mean distance of the CPG galaxies. The typical uncertainty in the observed colors is on the order of the bin sizes in Figures 4 and 5. Those galaxies with significantly higher uncertainties constitute a small fraction of the entire data base. Spiral galaxies show no consistent aperture dependence in their observed near-infrared colors (Aaronson 1977). Because the CPG sample is composed predominantly of spirals, there should be no significant effect on the mean colors relative to the mean colors of the control sample, nor on the dispersion in colors. Those galaxies with extremely red or blue colors shown in Figures 4 and 5 have radial velocities in the midrange of the CPG distribution (1000–5000 km s^{-1}).

We can examine the differences between the two distributions by applying the Kolmogorov-Smirnov two-sample test. This trial rejects the hypothesis that the two samples are drawn from populations with the same distribution, but only at the 90% significance level for the $J-K$ colors. The contrast is more dramatic in the $H-K$ distributions, which are confirmed to be different at the 99.5% significance level. The weak result found for the $J-H$ colors suggests that the statistics are dominated by the peaks of the distributions, which are similar, while the clear differences are in the tails.

One way to stress the contribution of the extremes of the populations is to define a simple two-state distribution. A galaxy will lie in either the "normal" range, as defined by the elliptical and S0 galaxies, or outside of it. The control sample then defines the probability of a noninteracting galaxy occupying either bin: $P(0.8 \leq J-K < 1.2) = 84/93 = 0.903$ and $P(J-K < 0.8$ and $J-K \geq 1.2) = 9/93 = 0.097$. Using Poisson statistics, the likelihood of producing the interacting galaxy distribution via a random sampling of the parent noninteracting population is found to be $< 10^{-5}$. If the upper boundary of the "normal" galaxy range is reduced to $J-K < 1.1$, the probability is still only $\sim 4 \times 10^{-5}$. These tests clearly illustrate that an excess of galaxies with aberrant near-infrared colors does exist in the selection of interacting galaxies. When comparing the full-color distributions of the two samples, however, that excess is seen to be a subtle one.

The $K-L$ color of a "normal" galaxy is 0.25 ± 0.05 mag. (Willner *et al.* 1984). Redward deviations from this can be interpreted as evidence for excess emission in the L band. Fifty percent of the CPG sample galaxies observed as a part of this work and by Joseph *et al.* (1984) have $K-L$ colors at least 1 σ level greater than 0.30 mag. This is in good agreement with the fraction of interacting galaxies observed to show red $K-L$ colors by Joseph *et al.* (1984). These authors interpreted the excesses as signs of starbursts induced by the interactions.

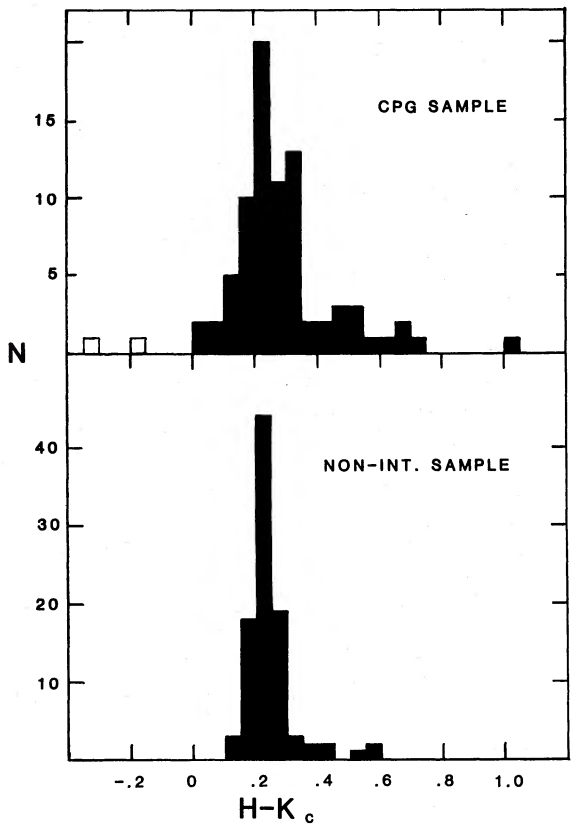

FIG. 5.—$H-K$ color distributions of the complete CPG sample of interacting galaxies (*top*) and noninteracting sample (*bottom*). Open boxes represent galaxy colors which have uncertainties of 0.07 mag or larger. All colors have been corrected for redshift and for reddening in our Galaxy.

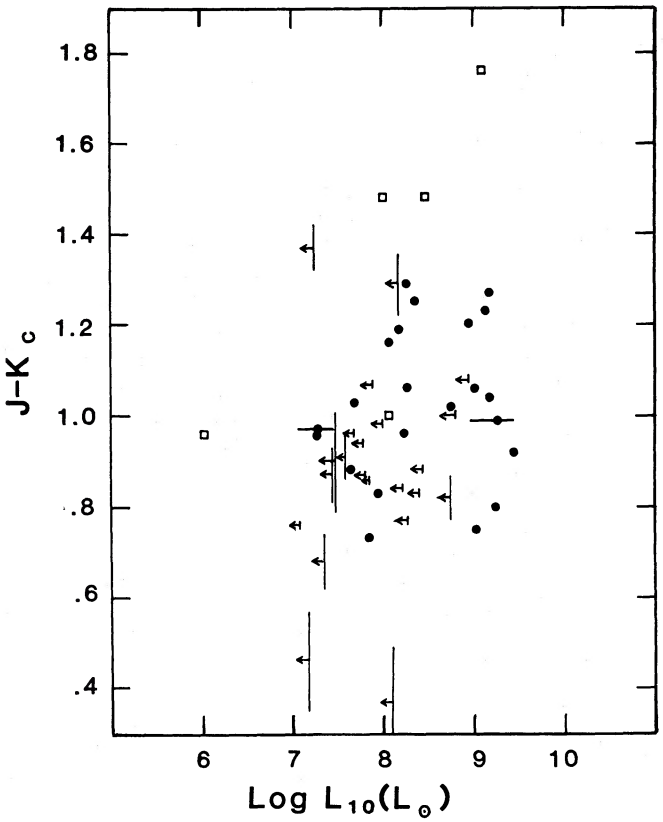

FIG. 6.—Corrected $J-K$ colors of the CPG sample plotted as a function of 10 μm luminosity. Open squares represent interacting galaxies taken from the control samples. Two sigma upper limits to the 10 μm luminosities are represented by arrows. Error bars are shown for those galaxies with uncertainties larger than 0.05 mag in $J-K$.

Because we did not make uniform 3.5 μm measurements of the CPG sample, and because there are not 3.5 μm measurements of the control sample galaxies, it is not possible to state for certain the interaction's role in producing the 3.5 μm excess. In light of the established prevalence of activity and the relation between the $K-L$ colors and 10 μm luminosity (see below), however, it is highly probable that the $K-L$ excesses are related to the galaxy encounters.

It is of interest to note that the nuclei with large 10 μm luminosities do not necessarily exhibit extreme $J-K$ colors. In Figure 6 we have plotted the 10 μm luminosities of the galaxies in our primary sample as a function of their corrected $J-K$ color. Again, upper limits to the 10 μm measurements are included only when their 1 σ level was 16 mJy or less. Although extremely red $J-K$ colors are not always associated with the extraluminous 10 μm emission, they do imply a very high probability of there being at least some nonstellar 10 μm emission. Eighty percent of the galaxies with $J-K \geq 1.2$ mag, and 83% with $J-K \geq 1.1$ mag were detected at 10 μm, as compared with the 45.5% detection for the sample overall. This disparity is significant because the mean radial velocity of the red interacting galaxies is similar to that of the sample as a whole.

In those sources with 10 μm excesses and normal $J-K$ colors, the nonstellar emission component must not be directly observable at wavelengths as short as 2 μm. The few available $K-L$ colors of the CPG galaxies do seem to correlate with the 10 μm luminosity, as can be seen in Figure 7. This suggests that the source of the 10 μm emission does contribute to the 3 μm light in the luminous sources. In the lower luminosity sources, however, even 3 μm measurements are not sensitive to the nonstellar emission which is so evident at the longer wavelengths.

V. CONCLUSIONS

Through small-aperture observations, we have examined the infrared emission from within the central kiloparsec or less of an unbiased sample of interacting pairs of galaxies. The 10 μm detection rate of the interacting CPG pairs as a function of redshift is consistently in excess of the detection rate expected for a distribution of galaxies with a Virgo-type luminosity function. At "higher" redshifts, this excess suggests that only interacting galaxies will be detected at 10 μm, and may account for the significant numbers of interacting systems present in infrared selected samples of galaxies.

The enhanced detection rates of the nuclei of interacting galaxies result from a 10 μm luminosity distribution which is substantially different from noninteracting galaxies. In addition to having a base poulation similar to that of the noninteracting galaxies, this distribution contains a secondary population which averages nearly 20 times more luminous than the mean of the noninteracting systems. Roughly one-fourth of the interacting galaxies observed at 10 μm, and nearly half of those detected, are members of this group.

Near-infrared photometry has shown that the $J-K$ and $H-K$ color distributions of the interacting galaxies resemble those of a large sample of noninteracting galaxies. However, a significant fraction of the interacting galaxies, roughly a factor of 3 larger than the fraction of noninteracting ones, have nuclear near-infrared colors outside the "normal" range.

The large-aperture observations of *IRAS* indicate that there is substantial extended 10 μm emission in at least half of the CPG sample. This supports the hypothesis of Larson and Tinsley (1978) that interactions can lead to global bursts of star formation. The enhanced galaxy-wide star formation is also manifested in the mean 80 μm luminosity of the CPG sample, which is $\sim$4 times larger than those of the Shapley-Ames gal-

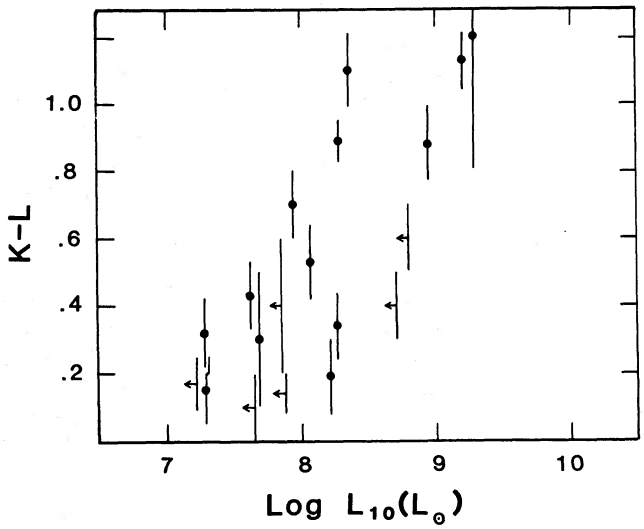

FIG. 7.—$K-L$ colors of the CPG sample plotted as a function of 10 μm luminosity. Two sigma upper limits to the 10 μm luminosities are represented by arrows.

axies surveyed by *IRAS* (de Jong *et al.* 1984) and the galaxies in the bright spiral sample of Rieke and Lebofsky (1978).

The presence of a luminous population of nuclei in interacting galaxies concurs with the results of Lonsdale, Persson, and Matthews (1984), who observed that, on average, the 10 μm luminosities of interacting galaxies are higher than those of noninteracting galaxies. Similarly, the near-infrared color distribution supports the conclusion of Joseph *et al.* (1984) that nuclear activity is common in interacting systems. The results presented here, however, better define the degree to which interactions are related to the presence of activity in the nuclei of galaxies. Comparisons with suitable control samples indicate that at least 50% of the galaxies in interacting pairs have infrared properties no different from those of noninteracting galaxies. Ultimately, it will be just as important to understand why interactions do not always induce activity.

Signs of abnormal nuclear activity are evident in a statistically significant fraction of interacting galaxies. These results indicate that interactions are capable of inducing and/or influencing not only galaxy-wide star formation, as noted by Larson and Tinsley (1978) and confirmed by the *IRAS* measurements discussed here, but also activity localized to the nuclei of the participant galaxies. In particular, the interactions are apparently responsible for phenomena which result in extremely luminous mid-infrared emission in certain nuclei. The identification of this extraluminous class of nuclei is of special interest because these nuclei may provide a possible link to other high-luminosity nuclear activity such as that found in Seyfert galaxies and QSOs. In addition, the luminous 10 μm galaxies may be part of the same class of object as the recently recognized "superstarburst" galaxies NGC 6240 and IC 4553 (Soifer *et al.* 1984*a*; Wright, Joseph, and Meikle 1984; Rieke *et al.* 1985). These objects, which harbor immensely luminous starbursts and possibly weak Seyfert nuclei, are apparently the result of severe galaxy mergers. Both galaxies lie at the upper end of the 10 μm luminosity distribution in Figure 3*a*, and probably represent the extreme results of the interaction process.

The authors would like to express their sincere gratitude to Drs. George Rieke, Marcia Lebofsky, Erick Young, John Stocke, and Bill Tifft for their invaluable advice and support during the course of this work. We also thank Dave Griep, Bill Golisch, Norm Purves, and John Hamilton for their assistance in obtaining parts of the data used here. This work was supported by grants from the National Science Foundation.

REFERENCES

Aaronson, M. 1977, Ph.D. thesis, Harvard University.
Aaronson, M., *et al.* 1982, *Ap. J. Suppl.*, **50**, 241.
Aaronson, M. A., and Mould, J. 1983, *Ap. J.*, **265**, 1.
Aaronson, M., and Olszchewski, E. W. 1984, *Nature*, **209**, 414.
Adams, T. F. 1977, *Ap. J. Suppl.*, **33**, 19.
Arp, H. C. 1966, *Ap. J. Suppl.*, **14**, 123.
Beichman, B. A., Neugebauer, G., Habing, H., Clegg, P. E., and Chester, T., eds. 1984, *IRAS Explanatory Supplement* (NASA Pub.).
Bothun G. D., Mould, J., Heckman, T., Balick, B., Schommer, R. A., and Kristian, J. 1982, *A.J.*, **87**, 1621.
Burstein, D., and Heiles, C. 1984, *Ap. J. Suppl.*, **54**, 33.
Campins, H. C., Rieke, G. H., and Lebofsky, M. J. 1985, *A.J.*, **90**, 896.
Condon, J. J., Condon, M. A., Gisler, G., and Pushell, J. J. 1982, *Ap. J.*, **252**, 102.
Condon, J. J., and Dressel, L. L. 1978, *Ap. J.*, **221**, 456.
Cutri, R. M., Rudy, R. J., Rieke, G. H., Tokunaga, A. T., and Willner, S. P. 1984, *Ap. J.*, **280**, 521.
Dahari, O. 1984*a*, *A.J.*, **89**, 966.
———. 1984*b*, preprint.
Davis, L. E. 1981, Ph.D. thesis, University of Toronto.
Davis, L. E., and Seaquist, E. R. 1983, *Ap. J. Suppl.*, **53**, 269.
de Jong, T., Clegg, P. E., Soifer, B. T., Rowan-Robinson, M., Habing, H. J., Houck, J. R., Gumann, H. H., and Raimond, E. 1984, *Ap. J.* (*Letters*), **278**, L67.
Dressel, L. L., and Condon, J. J. 1978, *Ap. J. Suppl.*, **36**, 53.
Elias, J. H., Frogel, J. A., Matthews, K., and Neugebauer, G. 1982, *A.J.*, **87**, 1029.
Feigelson, E. D., and Nelson, P. I. 1985, *Ap. J.*, **293**, 192.
Frogel, J. A., Persson, S. E., Aaronson, M., and Matthews, K. 1978, *Ap. J.*, **220**, 75.
Heckman, T. M., Bothun, G. D., Balick, B., and Smith, E. P. 1984, *A.J.*, **89**, 958.
Heckman, T. M., van Breugel, W. J. M., Miley, G. K., and Butcher, H. R. 1983, *A.J.*, **88**, 1077.
Hummel, E. 1981, *Astr. Ap.*, **96**, 111.
Hutchings, J. B., Crampton, D., Campbell, B., Duncan, D., and Glendenning, B. 1984, *Ap. J. Suppl.*, **55**, 319.
Joseph, R. D., Meikle, W. P. S., Robertson, N. A., and Wright, G. S. 1984, *M.N.R.A.S.*, **209**, 111.
Karachentsev, I. D. 1972, *Comm. Special Ap. Obs.*, **7**, 1.
Keel, W. C., Kennicutt, R. C., Hummel, E., and van der Hulst, J. M. 1985, *A.J.*, **90**, 708.
Kennicutt, R. C., Jr., and Keel, W. C. 1984, *Ap. J.* (*Letters*), **279**, L5.
Larson, R. B., and Tinsley, B. M. 1978, *Ap. J.*, **219**, 46.
Lebofsky, M. J., and Eisenhardt, P. E. 1985, *Ap. J.*, preprint.
Lonsdale, C. J., Neugebauer, G., and Soifer, B. T. 1984, *Bull. AAS*, **16**, 470.
Lonsdale, C. J., Persson, S. E., and Matthews, K. 1984, *Ap. J.*, **287**, 95.
Miller, R. H., and Smith, B. F. 1980, *Ap. J.*, **235**, 44.
Negroponte, J., and White, S. D. M. 1983, *M.N.R.A.S.*, **205**, 1009.
Rieke, G. H. 1976, *Ap. J.* (*Letters*), **206**, L15.
———. 1978, *Ap. J.*, **226**, 550.
Rieke, G. H., and Lebofsky, M. J. 1978, *Ap. J.* (*Letters*), **220**, L37.
———. 1985, *Ap. J.*, **288**, 618.
Rieke, G. H., Cutri, R. M., Black, J. H., Kailey, W. F., McAlary, C. W., Lebofsky, M. J., and Elston, R. 1985, *Ap. J.*, **290**, 116.
Rieke, G. H., Lebofsky, M. J., and Low, F. J. 1985, *A.J.*, **90**, 900.
Rieke, G. H., Lebofsky, M. J., Thompson, R. I., Low, F. J., and Tokunaga, A. T. 1980, *Ap. J.*, **238**, 24.
Scoville, N. Z., Becklin, E. E., Young, J. S., and Capps, R. W. 1983, *Ap. J.*, **271**, 512.
Soifer, B. T., Helou, G., Lonsdale, C. J., Neugebauer, G., Hacking, P., Houck, J.R., Rice, W., and Rowan-Robinson, M. 1984*a*, *Bull. AAS*, **16**, 470.
Soifer, B. T., *et al.* 1984*b*, *Ap. J.* (*Letters*), **278**, L71.
Stocke, J. T. 1977, Ph.D. thesis, University of Arizona.
Stocke, J. T., Tifft, W. G., and Kaftan-Kassim, M. A. 1978, *A.J.*, **83**, 322.
Stockton, A., and MacKenty, J. W. 1983, *Nature*, **305**, 678.
Sulentic, J. W. 1976, *Ap. J. Suppl.*, **32**, 195.
Tifft, W. G. 1982, *Ap. J. Suppl.*, **50**, 319.
Toomre, A., and Toomre, J. 1972, *Ap. J.*, **178**, 623.
Vorontsov-Velyaminov, B. A. 1959, *Atlas and Catalogue of Interacting Galaxies*, Part 1 (Moscow).
———. 1977, *Astr. Ap. Suppl.*, **28**, 1.
Wasilewski, A. J. 1983, *Ap. J.*, **272**, 68.
Willner, S. P., Ward, M., Longmore, A., Lawrence, A., Fabbiano, G., and Elvis, M. 1984, *Pub. A.S.P.*, **96**, 143.
Wright, G. S., Joseph, R. D., and Meikle, W. P. S. 1984, *Nature*, **309**, 430.

ROC M. CUTRI and CHRISTOPHER W. MCALARY: Steward Observatory, University of Arizona, Tucson, AZ 85721